

## Enthalpy of dilution in aqueous systems of single solutes ammonia, sodium sulfate and ammonium sulfate: Experimental results and modeling

Bernd Rumpf, Frank Weyrich, Gerd Maurer\*

*Lehrstuhl für Technische Thermodynamik, Universität Kaiserslautern, D-67653 Kaiserslautern, Federal Republic of Germany*

Received 14 April 1997; received in revised form 24 June 1997; accepted 1 July 1997

### Abstract

The enthalpy of dilution in the sodium sulfate–water, ammonium sulfate–water and ammonia–water systems was measured at temperatures from 313 to 373 K with a Calvet-type batch calorimeter using specially designed mixing cells. The mixing cells allow to pressurize the solutions. The formation of a gas phase during the experiments is thus avoided. Experimental results for the enthalpy of dilution are reported and compared to literature data and correlations. © 1997 Elsevier Science B.V.

*Keywords:* Ammonium sulfate; Aqueous solutions of ammonia; Enthalpy of dilution; Sodium sulfate

### 1. Introduction

The thermodynamic properties of aqueous solutions containing weak as well as strong electrolytes have to be determined in many applications. Typical examples are the cleaning of raw gases in power stations, the production of soda from aqueous solutions containing ammonia, carbon dioxide and sodium chloride or applications in the field of environment protection. Designing of separation equipment requires physico-chemical models in order to describe phase equilibria and caloric effects in such systems. Modeling phase equilibria and caloric effects in aqueous systems containing weak and strong electrolytes is a difficult task, due to chemical reactions in the liquid phase and ionic interactions, as well as due to the formation of solid phases. In most cases, process engineers are

primarily interested in phase equilibria and heats of vaporization in such systems whereas heats of dilution are often neglected in process design. However, for developing sound physico-chemical models, it is essential to separate the various contributions to enthalpy changes (i.e. from mixing, shifts in chemical reactions and due to the mass transfer over phase boundaries) as far as possible. Therefore, as part of an ongoing project dealing with experimental and theoretical work on the thermal properties of aqueous systems containing ammonia, sour gases – e.g. carbon dioxide – and strong electrolytes, enthalpies of dilution in the binary sodium sulfate–water, ammonium sulfate–water and ammonia–water systems were measured with a Calvet-type batch calorimeter at temperatures from 313 to 373 K. New mixing cells allowing to pressurize the solutions were developed. Experimental results are reported. Pitzer's model for the excess Gibbs energy was used to correlate the experimental data. Generally, the correlations agree

\*Corresponding author. Tel.: +49 631 205 2410; fax: +49 631 205 3835; e-mail: gmaurer@rhrk.uni-kl.de.

well with the experimental results. Together with published information on vapor–liquid equilibrium in these systems at one single temperature, parameter sets were determined which allow prediction of the vapor–liquid equilibrium over a wide range of temperatures and compositions.

## 2. Experimental section

A Calvet-type batch calorimeter (SETARAM MS 70, Lyon, France) was used for the experiments. In an experiment, two identical, pressurized mixing cells were placed in thermocouple columns inside the thermostatted calorimeter block. One cell was used as a reference cell, the other for the experiment. This differential arrangement compensated for the influence of the surroundings on the experiments. A caloric effect inside the cell resulted in a heat flow between the cell and the thermocouples, thus leading to a time-dependent thermovoltage signal. The signal was amplified and integrated by an integrator (SETARAM ITC). The integrated signal was directly proportional to the heat transferred between the cell and the thermocouple column. The proportionality constant was determined in separate calibration experiments (for details, cf. Hasse and Maurer [1] and Weyrich [2]).

For the volatile solutions investigated here, it was essential to avoid the presence of a gas phase in the cell. Therefore, mixing cells were developed which allow to pressurize the solutions. Fig. 1 shows a simplified scheme of a cell. The cell was divided into an upper and a lower chamber by a thin Teflon foil. In the top of the cell, a punching knife was mounted, which was used to cut the foil. Furthermore, a diaphragm bellows was mounted in the upper part of the cell. The inner side of the bellows was connected to a gas storage, maintained at constant pressure, thus the solution was pressurized.

The ammoniacal solution was prepared in the apparatus shown in Fig. 2. An evacuated cylinder sealed with a piston was filled with a known amount of water. A known amount of ammonia was added from a storage tank. The solution was pressurized to dissolve the gas completely in the liquid. To prepare the mixing cell, the lower chamber was filled with water (or the aqueous salt containing solution) with a syringe. The cell was connected to the filling system (cf. Fig. 2) and

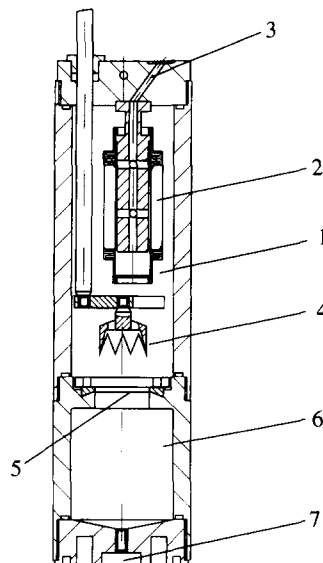


Fig. 1. Simplified scheme of the mixing cell: 1 – upper chamber; 2 – diaphragm bellows; 3 – connector for pressurization; 4 – punching knife; 5 – teflon foil; 6 – lower chamber; and 7 – connector for filling the lower chamber.

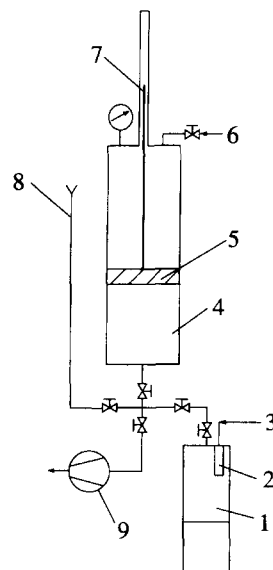


Fig. 2. Scheme of the apparatus for preparing and filling the solutions: 1 – mixing cell; 2 – diaphragm bellows; 3 – connector for pressurization; 4 – cylinder for preparing the solutions; 5 – piston; 6 – pressurization; 7 – level indicator; 8 – connector for filling the cylinder; and 9 – vacuum pump.

the upper chamber evacuated. The diaphragm bellows was pressurized to the same pressure as the ammoniac solution. Next, the upper part of the cell was filled with the ammoniac solution, thus avoiding evaporation of the liquid.

Two identically filled cells were placed into the thermocouple columns of the calorimeter. Both cells were pressurized to a pressure ca. 100 to 200 kPa above the boiling point pressure of the solution before or after mixing, whichever was less. After thermal equilibration, the mixing process in one of the cells was started by cutting the Teflon foil with the punching knife. During mixing, the diaphragm bellows compensated for density changes inside the cell, thus the (partial) evaporation of the liquid was avoided. However, due to the change of volume upon mixing, the heat determined in the experiment was not exactly equal to the enthalpy change resulting from the isobaric mixing process alone. For the mixing process, the first law of thermodynamics is

$$Q_{1,2} + W_{1,2} = \Delta U_{1,2}. \quad (1)$$

Approximating the isobaric, isothermal mixing process by a reversible change of state, that equation may be rewritten as

$$\Delta H_{1,2} = Q_{1,2} + \int_1^2 V dp. \quad (2)$$

Therefore, the measured heat  $Q_{1,2}$  has to be corrected by the last term in Eq. (2). That correction is calculated from the elastic behaviour of the diaphragm bellows together with the known densities of the solutions. Details of the calculation are given in Appendix A. For the experiments presented here,  $Q_{1,2}$  is typically ca. 10 to 200 J and the corrections are mostly smaller than 2 J.

Small errors could also arise due to frictional losses resulting from the movement of the punching knife when cutting the foil. That error was accounted for by pushing the knife again and measuring the heat transferred to the cell after that experiment. The heat dissipated due to the movement of the punching knife is typically smaller than 1 J.

At a fixed temperature, for each concentration of the dissolved species, at least two experiments with almost identical masses in the upper and lower cham-

ber of the mixing cell were performed. The results of those experiments in nearly all cases differed by less than 1 J.

Typically, ca. 28 g and 16 g of liquid were filled into the upper and lower chamber of the cell, respectively. The masses of the solutions were determined by weighing with a maximum uncertainty of  $\pm 0.08$  g. The uncertainty in determining the concentration of each component is smaller than 0.3%. Temperature was measured with calibrated platinum resistance thermometers with an uncertainty of ca.  $\pm 0.1$  K. A detailed calculation considering the propagation of all uncertainties (i.e. uncertainties in the concentrations of the dissolved species, in determining the masses filled into the cell, in determining the temperature and the heat transferred) showed that the absolute error in the enthalpy change upon mixing is below 1.5 J (for details cf. Weyrich [2]).

### 3. Substances

Ammonia ( $\geq 99.999$  mol%) was purchased from Messer-Griesheim, Ludwigshafen, Germany, and used without further purification. Sodium sulfate ( $\geq 99$  mass%) and ammonium sulfate ( $\geq 99.5$  mass%) were purchased from Merck GmbH, Darmstadt, Germany. The salts were degassed and dried under vacuum. Deionized water was further purified by vacuum distillation.

### 4. Results

#### 4.1. Test of procedure: Enthalpy of dilution in the $\text{Na}_2\text{SO}_4\text{-H}_2\text{O}$ system

To test the experimental equipment and procedures, the enthalpy of dilution in the sodium sulfate–water system was measured in the temperature range from 313 to 373 K. The results are summarized in Table 1 together with calculated numbers for the correction term (i.e. the integral in Eq. (2) (cf. Appendix A)). The concentration of the salt before dilution was ca. 0.5 mol/kg, 1 mol/kg and 1.5 mol/kg. Typically, ca. 17 g of the salt-containing solution were diluted with ca. 28 g of pure water. Measured enthalpies of dilution ranged from ca.  $-62$  to  $+46$  J.

Table 1  
Experimental results for the enthalpy of dilution in the sodium sulfate–water system

$T/K$ K	$m_{\text{Na}_2\text{SO}_4}^{(l)}$ (mol/kg)	$\tilde{m}^{(u)}$ / g	$\tilde{m}^{(l)}$ / g	$\Delta H_{1,2}$ / J	$\int V dp$ / J
313.2	0.500	27.583	16.901	4.7	0.37
313.2	0.500	27.424	16.900	4.7	0.37
313.2	0.500	27.309	16.953	4.4	0.37
313.2	1.001	27.253	17.820	23.1	0.17
313.2	1.001	27.963	17.690	22.8	0.18
313.2	1.500	28.101	18.742	46.2	-0.14
313.2	1.500	27.713	18.721	45.8	-0.14
313.2	1.500	27.371	18.761	46.0	-0.14
313.2	1.500	26.779	18.810	45.2	-0.15
333.4	0.500	27.588	16.970	-4.3	0.29
333.4	0.500	27.050	16.997	-4.0	0.28
333.4	1.000	27.938	17.884	-0.7	0.11
333.4	1.000	27.794	17.866	-0.8	0.11
333.4	1.500	27.552	18.758	4.9	-0.18
333.4	1.500	27.106	18.712	4.6	-0.18
353.1	0.500	25.343	16.909	-10.9	-0.12
353.1	0.500	25.593	16.932	-10.9	-0.12
353.2	1.000	27.160	18.015	-21.2	-0.29
353.1	1.000	25.661	17.746	-20.0	-0.27
353.1	1.000	25.880	17.726	-21.3	-0.27
353.1	1.500	25.385	18.681	-28.9	-0.50
353.1	1.500	25.681	18.650	-30.1	-0.51
373.4	0.500	25.569	16.391	-19.1	-0.77
373.4	0.500	25.302	16.308	-19.5	-0.75
373.3	1.000	26.481	17.369	-40.5	-0.95
373.4	1.000	26.627	17.414	-42.3	-0.96
373.4	1.500	24.766	18.398	-61.5	-1.06
373.4	1.500	25.149	18.262	-62.2	-1.08

During a series of measurements, neither the masses of the solutions filled into the upper and lower chambers of the mixing cells nor was the temperature held exactly constant. Therefore, for the graphical representation of the enthalpy of dilution, the original experimental data were interpolated to constant masses in the upper and lower chambers of the mixing cell and to a constant temperature (for details, cf. Weyrich [2]). However, only the original experimental data are presented in the tables.

In Fig. 3, the new results (interpolated to constant masses in the upper and lower chamber of the mixing cell and to a constant temperature) for the enthalpy of dilution in the binary sodium sulfate–water system are plotted vs. the molality of sodium sulfate in the lower

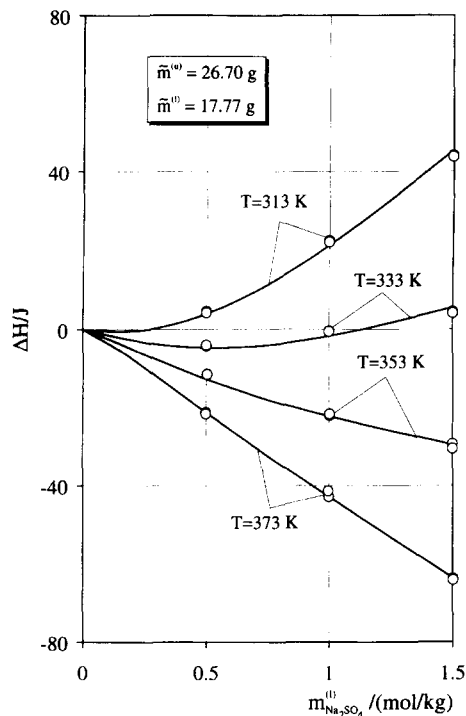


Fig. 3. Enthalpy of dilution in the sodium sulfate–water system. (○) – experimental results, this work; (—) – calculated results with the Pitzer model.

chamber before mixing. Furthermore, results calculated from the Pitzer [3] model with interaction parameters as taken from Rogers and Pitzer [4] are shown.

As can be seen from Fig. 3, at 313 K a mostly endothermic effect upon diluting aqueous solutions of sodium sulfate is observed. With increasing temperature, that endothermic effect turns into an exothermic effect. For example, at an initial molality of sodium sulfate of ca. 1.5 mol/kg, the enthalpy change upon diluting ca. 17.8 g of the aqueous, salt-containing solution with ca. 26.7 g of pure water is ca. 45 J at 313 K, whereas it is ca. -61 J at 373 K.

Experimental results for the enthalpy of dilution have been reported mostly as apparent molal enthalpies

$$L^\phi = \frac{H^E}{n_s} \quad (3)$$

of the solution before or after dilution. To allow a direct comparison to the literature data, apparent molal enthalpies were determined from the new data

as follows: For the isothermal mixing process, the enthalpy change is

$$\Delta H_{1,2} = n_s(L_2^\phi - L_1^\phi) \quad (4)$$

where subscripts 1 and 2 denote the state before and after mixing, respectively. As can be seen from Eq. (4), absolute values for the apparent molal enthalpy cannot be determined from experiments on the enthalpy of dilution. However, absolute numbers for  $L^\phi$  can be calculated from a model for the excess Gibbs energy of the solution. To compare the new experimental results to literature data, the Pitzer equation was used to calculate numbers for the apparent molal enthalpy after mixing. Numbers for  $L_1^\phi$  were then calculated from the experimental results for the enthalpy change by applying Eq. (4).

According to the Pitzer model, the excess Gibbs energy of an aqueous solution containing a single salt  $M_{\nu_1}X_{\nu_2}$  (salt molality:  $m_s$ ) is

$$\begin{aligned} \frac{G^E}{n_w M_w RT} = & f_1(I) + 2m_s^2 \nu_M \nu_X (\beta_{M,X}^{(0)} + \beta_{M,X}^{(1)}) \\ & + 2m_s^3 \nu_M^2 \nu_X \sqrt{\frac{z_M}{|z_X|}} C_{MX}^\phi \end{aligned} \quad (5)$$

where  $f_1, f_2$  are functions of ionic strength  $I$ ,  $\beta_{M,X}^{(0)}, \beta_{M,X}^{(1)}$  the binary interaction parameters and  $C_{MX}^\phi$  a ternary interaction parameter (for details, cf. Appendix B). The apparent molal enthalpy according to the Pitzer model is

$$\begin{aligned} L^\phi = & -RT^2 \left( \frac{1}{m_s} \frac{\partial f_1}{\partial T} + 2m_s \nu_M \nu_X \right. \\ & \times \left. \left[ \frac{\partial \beta_{M,X}^{(0)}}{\partial T} + \frac{\partial \beta_{M,X}^{(1)}}{\partial T} f_2(I) \right] \right) \\ & - 2RT^2 m_s^2 \nu_M^2 \nu_X \sqrt{\frac{z_M}{|z_X|}} \frac{\partial C_{MX}^\phi}{\partial T}. \end{aligned} \quad (6)$$

Interaction parameters  $\beta_{M,X}^{(0)}, \beta_{M,X}^{(1)}$  and  $C_{MX}^\phi$  for sodium sulfate were taken from Rogers and Pitzer [4] (cf. Appendix C). The calculation of  $f_1$  requires the dielectric constant of pure water which was calculated according to a correlation by Bradley and Pitzer [5] (cf. Appendix D).

In Fig. 4, the results for the apparent molal enthalpy calculated from the new experimental results for the enthalpy of dilution are plotted vs. the molality of

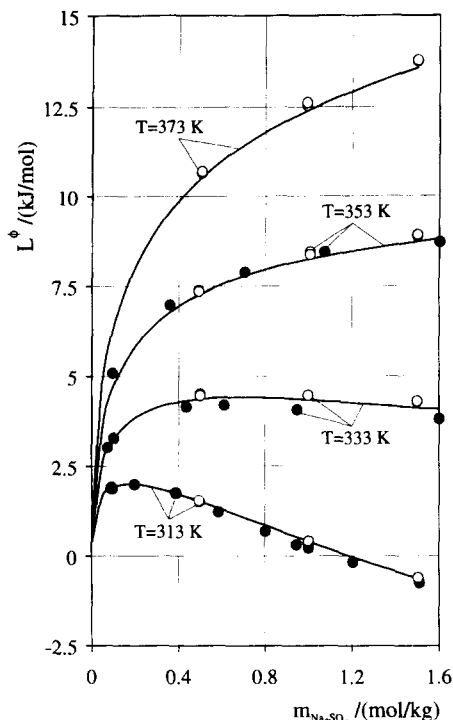


Fig. 4. Apparent molal enthalpy in the sodium sulfate–water system. (O) – experimental results, this work; (●) – experimental results, Snipes et al. [6]; and (—) – results calculated with the Pitzer model.

sodium sulfate before mixing. Furthermore, the data of Snipes et al. [6] and results calculated with the Pitzer model are shown. A good agreement between the new experimental data and those taken from the literature is observed, especially at 313 and 353 K. At those temperatures, the absolute deviation between the data of Snipes et al. and the new data is typically smaller than 0.15 kJ/mol. At 333 K, the data of Snipes et al. deviate systematically from the Pitzer equation whereas the new data agree well with that equation.

#### 4.2. Enthalpy of dilution in the $(NH_4)_2SO_4$ – $H_2O$ system

The enthalpy of dilution in the  $(NH_4)_2SO_4$ – $H_2O$  system was measured in the temperature range from 313 to 373 K. The results are summarized in Table 2. The salt molality before dilution ranged from ca. 1 to ca. 5 mol/kg. Typically, ca. 18 g of a salt-containing solution were diluted with ca. 26 g of pure water.

Table 2  
Experimental results for the enthalpy of dilution in the ammonium sulfate–water system

$T/$ K	$m_{(\text{NH}_4)_2\text{SO}_4}^{(i)}$ (mol/kg)	$\tilde{m}^{(u)}/$ g	$\tilde{m}^{(l)}/$ g	$\Delta H_{1,2}/$ J	$\int V dp /$ J
313.2	2.002	26.696	17.829	0.8	-0.79
313.2	2.002	28.028	17.907	0.6	-0.86
313.2	3.004	26.870	18.632	0.5	-0.87
313.2	3.004	28.912	18.873	0.1	-0.98
313.2	4.006	28.088	19.130	-13.3	-1.12
313.2	4.006	26.519	19.198	-13.8	-1.04
313.2	4.985	26.845	19.652	-33.7	-1.38
313.2	4.985	27.342	19.672	-33.3	-1.42
333.2	1.003	26.228	16.882	-15.7	-0.69
333.2	1.003	26.316	16.968	-15.7	-0.69
333.3	2.015	26.604	17.870	-30.9	-0.70
333.3	2.015	26.049	18.024	-31.4	-0.68
333.2	3.021	26.365	18.498	-52.8	-0.76
333.2	3.021	26.110	18.434	-51.6	-0.75
333.2	4.005	27.272	18.891	-82.8	-0.99
333.2	4.005	27.859	19.052	-83.0	-1.03
333.3	5.019	26.923	19.458	-123.6	-1.33
333.3	5.019	26.737	19.670	-123.2	-1.33
353.2	1.008	26.782	17.020	-28.3	-0.92
353.0	1.008	26.148	16.955	-27.7	-0.88
353.1	2.015	25.791	17.723	-60.9	-0.87
353.1	2.015	25.429	17.817	-60.9	-0.85
353.2	3.033	26.674	18.448	-101.2	-1.00
353.2	3.033	26.853	18.482	-103.4	-1.01
353.1	3.993	26.167	19.085	-147.2	-1.17
353.1	3.993	25.586	18.993	-148.7	-1.13
353.2	4.966	26.157	19.526	-199.7	-1.52
353.3	4.966	26.055	19.625	-201.5	-1.52
373.2	0.994	25.438	16.624	-41.1	-1.31
373.2	0.994	25.377	16.653	-41.0	-1.30
373.2	1.985	25.446	17.611	-85.9	-1.32
373.2	1.985	25.294	17.498	-86.1	-1.30
373.3	3.001	26.985	18.241	-145.7	-1.54
373.3	3.001	27.001	18.121	-147.5	-1.53
373.3	4.000	25.123	18.836	-202.0	-1.58
373.3	4.000	25.180	18.878	-205.2	-1.59
373.4	5.013	27.088	19.225	-279.6	-2.15
373.4	5.013	26.899	19.285	-280.5	-2.13

Measured enthalpy changes range from ca. 0 to -280 J, i.e. exothermic mixing behaviour is observed. The enthalpy (absolute number) decreases (increases) with rising temperature.

In Fig. 5, the experimental results for the enthalpy of dilution (again interpolated to constant masses in

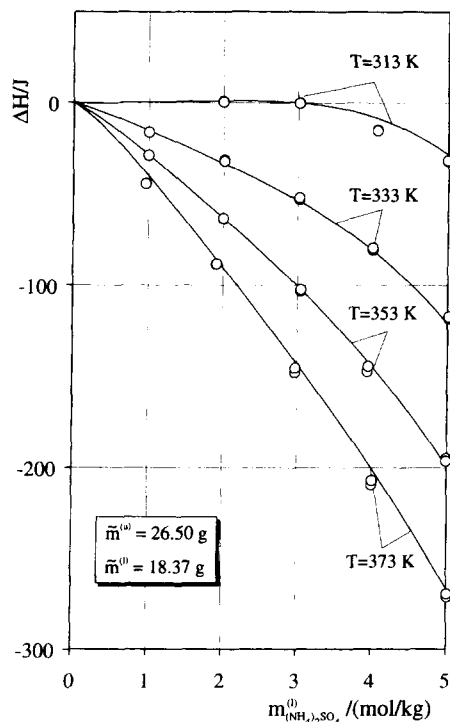


Fig. 5. Enthalpy of dilution in the ammonium sulfate–water system. (○) – experimental results, this work; and (—) – correlation, this work.

the upper and lower chamber of the mixing cell and to a constant temperature) are plotted vs. the molality of ammonium sulfate before dilution. Furthermore, the results of a correlation with the Pitzer model are shown (see below).

#### 4.3. Enthalpy of dilution in the $\text{NH}_3\text{--H}_2\text{O}$ system

The results for the enthalpy of dilution in the  $\text{NH}_3\text{--H}_2\text{O}$  system are summarized in Table 3. The ammonia molality before dilution ranged from ca. 6 up to ca. 18 mol/kg. Typically, ca. 25 g of an ammoniacal solution were diluted with ca. 16 g of pure water. Measured enthalpy changes ranged from ca. -29 to -300 J. As it is to be expected, only exothermic behaviour is observed. There is only a small influence of temperature on the enthalpy of dilution.

The experimental results for the enthalpy change upon dilution (interpolated to constant masses in the upper and lower chamber of the mixing cell and to a constant temperature) are plotted in Fig. 6 vs. the

Table 3

Experimental results for the enthalpy of dilution in the ammonia–water system

$T/\text{K}$	$m_{\text{NH}_3}^{(u)}/(\text{mol/kg})$	$\bar{m}^{(u)}/\text{g}$	$\bar{m}^{(l)}/\text{g}$	$\Delta H_{1,2}/\text{J}$	$\int V dp/\text{J}$
312.9	5.990	26.109	15.989	-30.6	0.04
312.9	5.990	26.193	15.975	-31.1	0.04
312.8	5.990	26.043	16.008	-30.4	0.04
312.8	12.198	25.180	16.042	-127.1	0.07
312.8	12.198	25.146	16.029	-128.7	0.07
312.2	17.998	24.657	16.000	-283.9	0.42
312.2	17.998	24.223	16.097	-285.8	0.41
333.6	5.990	25.936	16.001	-31.3	0.13
333.6	5.990	26.139	16.035	-31.1	0.13
333.6	5.990	26.391	15.947	-31.6	0.13
332.6	11.968	25.096	15.760	-126.0	0.19
332.6	11.968	24.843	15.756	-127.2	0.19
333.3	17.998	23.890	16.039	-293.6	0.56
333.2	17.998	24.069	16.028	-294.8	0.57
353.4	6.023	26.096	15.754	-30.9	0.02
353.4	6.023	26.012	15.784	-31.7	0.02
352.7	11.916	25.617	15.780	-132.2	0.14
353.3	11.916	25.827	15.966	-134.3	0.14
353.3	11.916	26.205	15.826	-135.0	0.15
353.1	17.544	24.177	15.968	-290.2	0.66
353.0	17.544	23.455	16.000	-287.6	0.64
373.2	5.794	26.028	15.383	-29.4	-0.24
373.3	6.050	24.380	15.746	-32.4	-0.24
373.3	12.143	24.997	15.498	-136.2	-0.07
373.3	12.143	25.169	15.573	-134.7	-0.07
373.3	17.715	24.051	15.658	-304.4	0.58
373.3	17.715	23.947	15.505	-303.0	0.58

molality of ammonia before dilution together with the results of a correlation (see below).

## 5. Modeling

### 5.1. The $(\text{NH}_4)_2\text{SO}_4\text{-H}_2\text{O}$ system

For an aqueous system containing a single salt, the Pitzer model for the excess Gibbs energy requires three interaction parameters (cf. Eq. (5)). Thus, to correlate the new results for the enthalpy of dilution in the ammonium sulfate–water system, the temperature derivatives of the interaction parameters  $\beta_{\text{NH}_4^+, \text{SO}_4^{2-}}^{(0)}$ ,  $\beta_{\text{NH}_4^+, \text{SO}_4^{2-}}^{(1)}$  and  $C_{(\text{NH}_4)_2\text{SO}_4}^\phi$  were fitted to

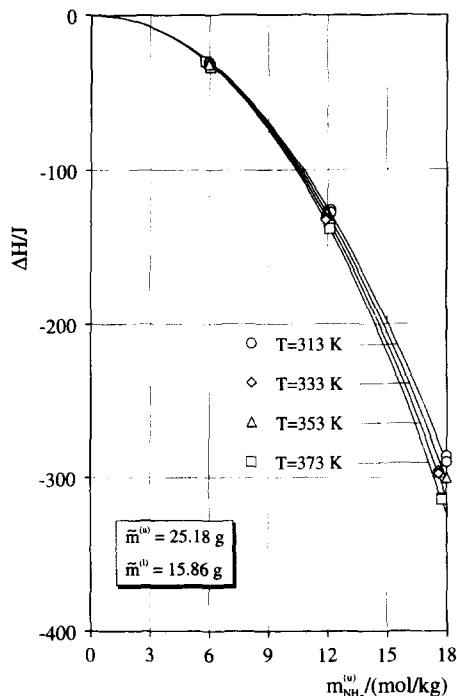


Fig. 6. Enthalpy of dilution in the ammonia–water system. (○, ◇, △, □) – experimental results, this work; and (—) – correlation, this work.

the results for the enthalpy of dilution. The influence of temperature on the interaction parameters was described by an empirical equation:

$$f(T) = q_0 + \frac{q_1}{T/K} + q_2 \ln(T/K) + q_3(T/K). \quad (7)$$

Parameters  $q_1$  to  $q_3$  were determined from the new experimental data for the enthalpy of dilution, parameters  $q_0$  from numbers for  $\beta_{\text{NH}_4^+, \text{SO}_4^{2-}}^{(0)}$ ,  $\beta_{\text{NH}_4^+, \text{SO}_4^{2-}}^{(1)}$  and  $C_{(\text{NH}_4)_2\text{SO}_4}^\phi$  at 298.15 K as given by Pitzer [7]. The resulting set of parameters is given in Table 4. With that parameter set, the new data for the enthalpy of dilution are correlated with an average absolute deviation of 2 J (cf. Fig. 5).

The new correlation can also be used to calculate other properties, e.g. the pressure above and the osmotic coefficient of aqueous solutions of ammonium sulfate (for details, see further on). Figs. 7 and 8 show a comparison between calculated and experi-

Table 4  
Interaction parameters to describe phase equilibria and caloric effects in aqueous systems containing ammonium sulfate

Parameter	$q_0$	$q_1$	$q_2$	$q_3$
$\beta_{\text{NH}_4^+, \text{SO}_4^{2-}}^{(0)}$	17.79893	-589.017	-2.979609	$4.005157 \times 10^{-3}$
$\beta_{\text{NH}_4^+, \text{SO}_4^{2-}}^{\text{NH}_4^+}$	766.00	-23129.6	-130.631	0.189579
$C_{(\text{NH}_4)_2\text{SO}_4}$	$-4.203152 \times 10^{-3}$	3.39601	$5.78395 \times 10^{-3}$	—

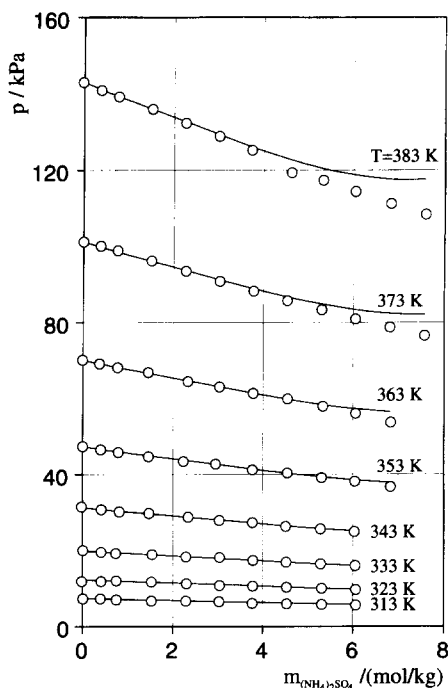


Fig. 7. Total pressure above aqueous solutions of ammonium sulfate. (○) – experimental results, Nikolski [8]; and (—) – prediction from the calorimetric results of this work and interaction parameters at 298.15 K as given by Pitzer [7].

mental results. In Fig. 7, the experimental results of Nikolski [8] for the total pressure are compared to predictions from the present work at temperatures between 313 and 383 K and salt molalities of up to ca. 8 mol/kg. The predictions agree with the experimental data within ca. 1% at ammonium sulfate concentrations of up to ca. 5 mol/kg, i.e. up to the maximum salt concentration investigated in the present work. However, at higher salt concentrations, larger differences are observed and calculated pressures are always larger than observed experimentally. The deviation between predicted and measured pressures increases with temperature and ammonium

sulfate molality to ca. 8% at 383 K and ca. 8 mol  $(\text{NH}_4)_2\text{SO}_4/\text{kg}$  of water. It was also attempted to include this total pressure data into the determination of the binary and ternary interaction parameters. However, no significant improvement could be achieved. The failure might be due either to some inconsistencies in the experimental data or to the extension of the Pitzer model to a very high ionic strength (in an aqueous solution containing eight moles of  $(\text{NH}_4)_2\text{SO}_4$  per kilogram of water, the ionic strength is 24 mol/kg!). The results of Clegg et al. [9] for the osmotic coefficient, namely

$$\phi = \frac{-\ln a_w}{M_w(\nu_M + \nu_X)m_s} \quad (8)$$

of aqueous solutions of ammonium sulfate at 298.15 K and 323.15 K may be used to support either one (or both) suspicions. The experimental data of Clegg et al. are compared with predictions in Fig. 8. At high ammonium sulfate molalities, calculated osmotic coefficients are larger than the experimental results (e.g. at  $m_s = 6$  mol/kg by ca. 6 and 1.6% at 298 and 323 K, respectively). However, lower osmotic coefficients correspond to higher vapor pressures. Thus, the signs of the differences between calculated and experimental data are different for the data of Clegg et al. and those of Nikolski. But the results of Clegg et al. can also be used to support the suspected problems in regard to the Pitzer model. Clegg et al. also described their experimental results for the osmotic coefficient with the Pitzer model, but they introduced an influence of the ionic strength on the parameter describing ternary interactions. Obviously, additional experimental results are required especially at high salt concentrations over a wide range of temperatures to arrive at an unambiguous decision on the reason for the differences between calculated and measured pressures and osmotic coefficients of aqueous solutions of ammonium sulfate at high salt concentrations.

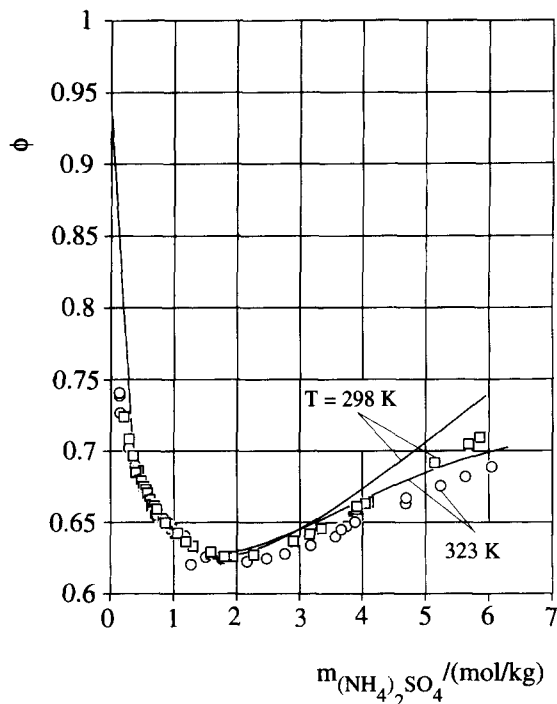


Fig. 8. Osmotic coefficients in the ammonium sulfate–water system. (O, □) – experimental results, Clegg et al. [9]; and (—) – prediction from the calorimetric results of this work and interaction parameters at 298.15 K as given by Pitzer [7].

### 5.2. The $\text{NH}_3\text{--H}_2\text{O}$ system

To correlate the new results for the enthalpy of dilution in the ammonia–water system, a similar procedure as described before was applied. In the concentration range investigated here, the protolysis of ammonia can be neglected. Two interaction parameters ( $\beta_{\text{NH}_3,\text{NH}_3}^{(0)}$  and  $\tau_{\text{NH}_3,\text{NH}_3,\text{NH}_3}$ , cf. Appendix B) are required to describe caloric effects and phase equilibria in the  $\text{NH}_3\text{--H}_2\text{O}$  system with the Pitzer equation. The temperature derivatives of both interaction parameters were fitted to the new data (cf. Table 3) for the enthalpy of dilution. The influence of temperature on both parameters was approximated by Eq. (7); however, it proved sufficient to neglect the last term (i.e.  $q_3 = 0$ ). Parameters  $q_1$  and  $q_2$  were fitted to the experimental results for the enthalpy of dilution. The remaining parameters  $q_0$  were determined from vapor–liquid equilibrium data for the ammonia–water system as follows: The composition of the vapor phase

was calculated applying extended Raoult's law for water (solvent)

$$py_w \phi_w'' = p_w^s \phi_w^s \exp\left(\frac{v_w(p - p_w^s)}{R}\right) a_w \quad (9)$$

and extended Henry's law for ammonia (solute)

$$py_{\text{NH}_3} \phi_{\text{NH}_3}'' = H_{\text{NH}_3,w}^{(m)}(T, p_w^s) \times \exp\left(\frac{v_{\text{NH}_3,w}^\infty(p - p_w^s)}{RT}\right) m_{\text{NH}_3} \gamma_{\text{NH}_3}^{(m)} \quad (10)$$

Henry's constant for ammonia was taken from Rumpf and Maurer [10]. The fugacity coefficients of water and ammonia were calculated from the virial equation of state with second virial coefficients also taken from Rumpf and Maurer [10]. The vapor pressure and density of pure water were calculated from the equations of Saul and Wagner [11] (cf. Appendix E). The partial molar volume of ammonia at infinite dilution in water was calculated according to the procedure by Brelvi and O'Connell [12]. Numbers for the interaction parameters  $\beta_{\text{NH}_3,\text{NH}_3}^{(0)}$  and  $\tau_{\text{NH}_3,\text{NH}_3,\text{NH}_3}$  were then determined by fitting to the isothermal vapor–liquid equilibrium data of Smolen et al. [13] at 353 K, thus resulting in numbers for the parameters  $q_0$  in Eq. (7). The resulting set of parameters is given in Table 5.

In Fig. 9, the data of Smolen et al. [13] for the total pressure above aqueous ammoniacal solutions are plotted versus the molality of ammonia dissolved in the liquid phase. Furthermore, results calculated with the Pitzer model are shown. Except for 353 K, the calculated isotherms are predictions. A good agreement between the experimental and predicted total pressures is observed, although the temperature range of the vapor–liquid equilibrium data (293 to 413 K) is by far larger than that of the new data for the enthalpy of dilution (313 to 373 K). The average and maximum relative deviation is 0.8 and 3%, respectively. The

Table 5  
Interaction parameters to describe phase equilibria and caloric effects in the ammonia–water system

Parameter	$q_0$	$q_1$	$q_2$
$\beta_{\text{NH}_3,\text{NH}_3}^{(0)}$	−0.0197	9.864	—
$\tau_{\text{NH}_3,\text{NH}_3,\text{NH}_3}$	$5.539 \times 10^{-3}$	−1.1789	$-8.61 \times 10^{-4}$

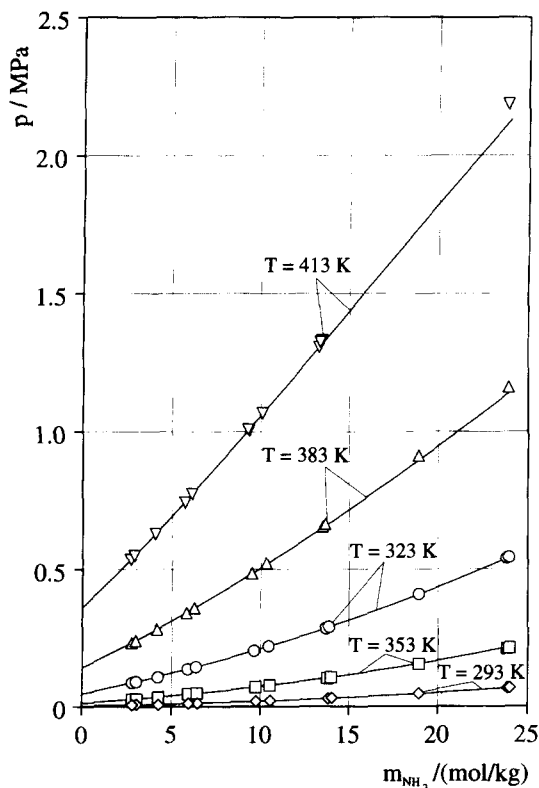


Fig. 9. Total pressure above aqueous solutions of ammonia. ( $\diamond$ ,  $\square$ ,  $\circ$ ,  $\triangle$ ,  $\nabla$ ) – experimental results, Smolen et al. [13]; and (—) – prediction, this work.

partial pressures of ammonia and water are predicted with average relative deviations of 0.8 and 2.7%, respectively.

No experimental results for the enthalpy of dilution of aqueous solutions of ammonia in the temperature and concentration range investigated here have been reported in the literature. However, some results for the heat effect observed when pure, liquid ammonia is mixed with water have been reported, e.g. by Macriss et al. [14], Scatchard et al. [15] and Staudt [16]. A comparison between that literature data and the new results requires a transformation of reference states, i.e. an extrapolation of the experimental results either to pure water or to pure ammonia. Such an extrapolation results in large uncertainties in the differences of reference state enthalpies. The uncertainties are too large to allow for a reasonable comparison between the different data sets (cf. Weyrich [2]).

## 6. Conclusions

The enthalpy change accompanying the isothermal, isobaric dilution of aqueous solutions of the single solutes sodium sulfate, ammonium sulfate and ammonia were determined by batch calorimetry at temperatures between 313 and 373 K and solute concentrations of up to about 1.5 ( $\text{Na}_2\text{SO}_4$ ), 5 ( $(\text{NH}_4)_2\text{SO}_4$ ) and 18 ( $\text{NH}_3$ ) mol/kg. The experimental results are compared with literature data ( $\text{H}_2\text{O} + \text{Na}_2\text{SO}_4$ ) and correlated using Pitzer's model for the Gibbs excess energy. The correlations are also used to predict the vapor–liquid equilibrium (i.e. vapor pressure and osmotic coefficients in the  $\text{H}_2\text{O} + (\text{NH}_4)_2\text{SO}_4$  system and total pressure and partial pressures in the  $\text{NH}_3 + \text{H}_2\text{O}$  system). With the exception of the vapor pressure above aqueous solutions of  $(\text{NH}_4)_2\text{SO}_4$  at high salt concentration, the predictions agree with the experimental data within the experimental uncertainty.

## 7. Nomenclature

$A_B$	effective cross sectional area of the diaphragm bellows
$A_\phi$	Debye–Hückel parameter
$a_i$	activity of component $i$
$a_1 \dots a_6$	constants in the equation for the vapor pressure of pure water
$b_1 \dots b_6$	constants in the equation for the density of pure water
$b$	constant in modified Debye–Hückel expression
$B(T), C(T)$	functions in the expression for the dielectric constant of pure water
$a_i, b_i, c_i$	constants in Eq. (A.8)
$C^\phi$	third virial coefficient in Pitzer's equation
$D$	relative dielectric constant of water
$D$	function of temperature (cf. Eq. (C.6))
$e$	charge of proton
$f$	function for the temperature dependence of an interaction parameter
$f_1, f_2, f_3$	functions in Pitzer's equation
$G^E$	excess Gibbs energy
$H$	enthalpy

$H_{i,w}^{(m)}$	Henry's constant for the solubility of gas $i$ in pure water (on molality scale)
$H^E$	excess enthalpy
$I$	ionic strength (on molality scale)
$k$	Boltzmann constant
$k_B$	force constant of the diaphragm bellows
$l$	elongation of diaphragm bellows
$L^\phi$	apparent molal enthalpy
$M_w$	molar mass of water in kg/mol, i.e. 0.018 kg/mol
$m_i$	molality of component $i$
$\tilde{m}_i$	mass of component $i$
$n_i$	number of moles of component $i$
$N_A$	Avogadro's number
$p$	total pressure
$Q$	heat
$q_i$	coefficient for the temperature dependence of an interaction parameter
$R$	universal gas constant
$T$	absolute temperature
$U$	internal energy
$U_1 \dots U_9$	constants in the expression for the dielectric constant of pure water
$V$	volume
$v$	partial molar volume
$W$	work
$x$	variable in Pitzer's equation
$y$	mole fraction in vapor
$z_i$	number of charges of component $i$

### 7.1. Greek letters

$\alpha$	constant in Pitzer's equation
$\beta^{(0)}, \beta^{(1)}$	binary interaction parameters in Pitzer's equation
$\gamma$	activity coefficient
$\Delta$	difference
$\epsilon_0$	vacuum permittivity
$\nu_M, \nu_X$	number of cations and anions in salt MX
$\rho$	mass density
$\tau_{i,j,k}$	ternary interaction parameter in Pitzer's equation
$\theta$	reduced temperature (cf. Eq. (E.3))
$\varphi$	fugacity coefficient
$\phi$	osmotic coefficient

### 7.2. Subscripts

c	critical
$i, j, k$	component $i, j, k$
MX	salt MX
M	cation M
X	anion X
R	reference
w	water
s	salt
0	reference
1	state before mixing
2	state after mixing

### 7.3. Superscripts

(l)	lower chamber
s	saturation
(u)	upper chamber
(m)	normalized to infinite dilution, i.e. $m_i = 1$ mol/kg in water for concentration, but $m_i \rightarrow 0$ in water for interactions
$\infty$	infinite dilution
'	liquid phase
"	gas phase

### Acknowledgements

Financial support of this investigation by the Deutsche Forschungsgemeinschaft, Bonn is gratefully acknowledged.

### Appendix A

*Details on the procedure applied to calculate the enthalpy change upon dilution from the direct experimental results*

To calculate the enthalpy change upon dilution from the experimental results for the heat measured in an experiment (cf. Eq. (2)), the following procedure was applied: Let  $V_1$  be the volume of the solution before mixing where the elongation of the diaphragm bellows is  $l_1$ . Then, at an arbitrary elongation  $l$ , the volume of the solution is

$$V = V_1 - A_B(l - l_1) \quad (\text{A.1})$$

where  $A_B$  is the effective cross sectional area of the

Table 6

Densities in the NH<sub>3</sub>–H<sub>2</sub>O, (NH<sub>4</sub>)<sub>2</sub>SO<sub>4</sub>–H<sub>2</sub>O and Na<sub>2</sub>SO<sub>4</sub>–H<sub>2</sub>O binary systems: Coefficients of Eq. (A.8)

System source of data	NH <sub>3</sub> –H <sub>2</sub> O D'Ans, Lax [17]	Na <sub>2</sub> SO <sub>4</sub> –H <sub>2</sub> O Landolt–Börnstein [18]	(NH <sub>4</sub> ) <sub>2</sub> SO <sub>4</sub> –H <sub>2</sub> O Landolt–Börnstein [18]
$a_1$	1.1479	1.1182	1.1550
$a_2$	$-5.0106 \times 10^{-4}$	$-4.1329 \times 10^{-4}$	$-4.9860 \times 10^{-4}$
$b_1$	$-1.4227 \times 10^{-3}$	$1.6708 \times 10^{-1}$	$5.8814 \times 10^{-2}$
$b_2$	$-1.8524 \times 10^{-5}$	$-1.3825 \times 10^{-4}$	$1.0640 \times 10^{-5}$
$c_1$	$-7.3882 \times 10^{-5}$	$-1.7848 \times 10^{-2}$	$-3.2702 \times 10^{-3}$
$c_2$	$6.1781 \times 10^{-7}$	$2.9763 \times 10^{-5}$	$-5.9800 \times 10^{-7}$

diaphragm bellows. Assuming Hooke's law for the elastic behaviour of the diaphragm bellows, the difference between the pressure in the cell  $p_i$  and the pressure  $p_0$  is:

$$p_i = p_0 - \frac{k_B}{A_B}(l - l_0) \quad (\text{A.2})$$

where  $l_0$  is the elongation of the diaphragm bellows when there is no pressure difference across the bellows. From Eq. (A.2), it follows

$$dp_i = -\frac{k_B}{A_B}dl. \quad (\text{A.3})$$

Inserting Eqs. (A.1) and (A.3) into Eq. (2) results in

$$\int_1^2 V dp = -\frac{V_1 k_B}{A_B} \left( \frac{V_2 - V_1}{A_B} \right) + \frac{1}{2} k_B \left( \frac{V_2 - V_1}{A_B} \right)^2. \quad (\text{A.4})$$

The volumes of the solutions before and after mixing may be expressed by the masses and densities before and after mixing:

$$V_1 = \frac{\tilde{m}^{(u)}}{\varrho^{(u)}} + \frac{\tilde{m}^{(l)}}{\varrho^{(l)}} \quad (\text{A.5})$$

$$V_2 = \frac{\tilde{m}^{(u)} + \tilde{m}^{(l)}}{\varrho_2}. \quad (\text{A.6})$$

Hence, Eq. (A.4) can be rewritten:

$$\int_1^2 V dp = -\frac{k_B}{A_B^2} \left[ \left( \frac{\tilde{m}^{(u)}}{\varrho^{(u)}} + \frac{\tilde{m}^{(l)}}{\varrho^{(l)}} \right) \times \left( \frac{\tilde{m}^{(u)} + \tilde{m}^{(l)}}{\varrho_2} - \frac{\tilde{m}^{(u)}}{\varrho^{(u)}} - \frac{\tilde{m}^{(l)}}{\varrho^{(l)}} \right) - \frac{1}{2} \left( \frac{\tilde{m}^{(u)} + \tilde{m}^{(l)}}{\varrho_2} - \frac{\tilde{m}^{(u)}}{\varrho^{(u)}} - \frac{\tilde{m}^{(l)}}{\varrho^{(l)}} \right)^2 \right]. \quad (\text{A.7})$$

The following empirical equations were used to calculate the densities of the aqueous solutions:

$$\frac{\varrho'(T, m_i)}{\text{g/cm}^3} = (a_1 + a_2(T/K)) + (b_1 + b_2(T/K))m_i/(\text{mol kg}^{-1}) + (c_1 + c_2(T/K))(m_i/(\text{mol kg}^{-1}))^2. \quad (\text{A.8})$$

Coefficients  $a_i$  to  $c_i$  were fitted to experimental results for the density in the sodium sulfate–water, ammonium sulfate–water and ammonia–water systems. The resulting coefficients as well as the literature sources of the experimental data are given in Table 6.

## Appendix B

### Brief outline of Pitzer's model

Pitzer's [3] equation for the excess Gibbs energy of an aqueous, salt-containing system is

$$\frac{G^E}{RTn_w M_w} = f_1(I) + \sum_{i \neq w} \sum_{j \neq w} m_i m_j (\beta_{ij}^{(0)} + \beta_{ij}^{(1)} f_2(x)) + \sum_{i \neq w} \sum_{j \neq w} \sum_{k \neq w} m_i m_j m_k \tau_{i,j,k} \quad (\text{B.1})$$

where  $\beta_{ij}^{(0)}$ ,  $\beta_{ij}^{(1)}$  and  $\tau_{i,j,k}$  are binary and ternary interaction parameters, respectively. The function  $f_1(I)$  is a modified Debye–Hückel term

$$f_1(I) = -A_\phi \frac{4I}{b} \ln(1 + b\sqrt{I}) \quad (\text{B.2})$$

where  $I$  is the ionic strength

$$I = \frac{1}{2} \sum_i m_i z_i^2 \quad (\text{B.3})$$

and  $b = 1.2$  (kg/mol)<sup>1/2</sup>.  $A_\phi$  is the Debye–Hückel parameter for the osmotic coefficient

$$A_\phi = \frac{1}{3} \sqrt{2\pi N_A \frac{\rho_w'}{1000} \left( \frac{e^2}{4\pi\epsilon_0 D k T} \right)^{3/2}}. \quad (\text{B.4})$$

The function  $f_2$  is defined as

$$f_2(x) = \frac{2}{x^2} (1 - (1+x)e^{-x}) \quad (\text{B.5})$$

where  $x = \alpha\sqrt{I}$ . For the salts considered here,  $\alpha = 2.0$  (kg/mol)<sup>1/2</sup>.

Differentiation of Eq. (B.1) yields the activity coefficient of the dissolved species  $i$ :

$$\begin{aligned} \ln \gamma_i^{(m)} = & -A_\phi z_i^2 \left( \frac{\sqrt{I}}{1+b\sqrt{I}} + \frac{2}{b} \ln(1+b\sqrt{I}) \right) \\ & + 2 \sum_{j \neq w} m_j (\beta_{ij}^{(0)} + \beta_{ij}^{(1)} f_2(x)) \\ & - z_i^2 \sum_{j \neq w} \sum_{k \neq w} m_j m_k \beta_{ijk}^{(1)} f_3(x) \\ & + 3 \sum_{j \neq w} \sum_{k \neq w} m_j m_k \tau_{ij,k} \end{aligned} \quad (\text{B.6})$$

where  $f_3$  is defined as

$$f_3(x) = \frac{1}{I x^2} \left( 1 - \left( 1 + x + \frac{x^2}{2} \right) e^{-x} \right). \quad (\text{B.7})$$

The activity of water follows from the Gibbs–Duhem equation

$$\begin{aligned} \ln a_w = & M_w \left( 2A_\phi \frac{I^{1.5}}{1+b\sqrt{I}} - \sum_{i \neq w} \sum_{j \neq w} m_i m_j \right. \\ & \times \left. \left( \beta_{ij}^{(0)} + \beta_{ij}^{(1)} e^{-x} \right) \right) - M_w \\ & \times \left( 2 \sum_{i \neq w} \sum_{j \neq w} \sum_{k \neq w} m_i m_j m_k \tau_{ij,k} - \sum_{i \neq w} m_i \right). \end{aligned} \quad (\text{B.8})$$

For systems containing a single salt  $M_{\nu_+} X_{\nu_-}$ , the binary and ternary parameters involving two or more species of the same sign of charge are usually neglected. The ternary parameters  $\tau_{M,X,X}$  and  $\tau_{M,M,X}$  are usually reported as third virial coefficients  $C^\phi$  for

the osmotic coefficient. Instead of rewriting Eqs. (B.6) and (B.8) in terms of  $C^\phi$ , we preferred to set  $\tau_{M,X,X}$  to zero and calculated the ternary parameters  $\tau_{M,M,X}$  from numbers reported for  $C^\phi$ :

$$2 : 1 \text{ salt} : \quad \tau_{M,M,X} = \frac{\sqrt{2}}{6} C^\phi \quad (\text{B.9})$$

## Appendix C

### Interaction parameters for Pitzer's equation

The following section reports relations for the temperature dependence of the interaction parameters for sodium sulfate as given by Rogers and Pitzer [4].  $T$  is the temperature in Kelvin and  $T_R = 298.15$  K.

$$\begin{aligned} \beta^{(0)} = & \beta^{(0)}(T_R) - A \left( \frac{1}{T} - \frac{1}{T_R} \right) + q_5 (T^2 - T_R^2) \\ & + q_6 (T - T_R) + q_7 \ln \left( \frac{T}{T_R} \right) \\ & - q_8 \left( \frac{1}{T} - \frac{1}{T_R} \right) + q_8 \left( \frac{1}{T - 263} - \frac{1}{T_R - 263} \right) \end{aligned} \quad (\text{C.1})$$

$$\begin{aligned} A = & T_R^2 \left( \frac{\partial \beta^{(0)}}{\partial T} \right)_{T=T_R} - 2q_5 T_R^3 - q_6 T_R^2 - q_7 T_R \\ & + 526q_8 \left( \frac{1}{T_R - 263} + \frac{263}{2(T_R - 263)^2} \right) \end{aligned} \quad (\text{C.2})$$

$$\begin{aligned} \beta^{(1)} = & \beta^{(1)}(T_R) - B \left( \frac{1}{T} - \frac{1}{T_R} \right) + q_9 (T^2 - T_R^2) \\ & + q_{10} (T - T_R) + q_{11} \ln \left( \frac{T}{T_R} \right) \\ & - q_{12} \left( \frac{1}{T} - \frac{1}{T_R} \right) \\ & + q_{12} \left( \frac{1}{T - 263} - \frac{1}{T_R - 263} \right) \\ & - 680q_{13} \left( \frac{1}{(T - 680)T} - \frac{1}{(T_R - 680)T_R} \right) \end{aligned} \quad (\text{C.3})$$

$$B = T_R^2 \left( \frac{\partial \beta^{(1)}}{\partial T} \right)_{T=T_R} - 2q_9 T_R^3 - q_{10} T_R^2 - q_{11} T_R$$

$$+ 526q_{12} \left( \frac{1}{T_R - 263} + \frac{263}{2(T_R - 263)^2} \right)$$

$$- 1360q_{13} \left( \frac{680}{2(T_R - 680)^2} - \frac{1}{680 - T_R} \right) \quad (\text{C.4})$$

$$C^\phi = C^\phi(T_R) - D \left( \frac{1}{T} - \frac{1}{T_R} \right) + q_{14}(T - T_R)$$

$$+ 263q_{15} \left( \frac{1}{(T - 263)T} - \frac{1}{(T_R - 263)T_R} \right) \quad (\text{C.5})$$

$$D = T_R^2 \left( \frac{\partial C^\phi}{\partial T} \right)_{T=T_R} - q_{14} T_R^2$$

$$+ 526q_{15} \left( \frac{1}{T_R - 263} + \frac{1}{2(T_R - 263)^2} \right) \quad (\text{C.6})$$

$$\begin{aligned} \beta^{(0)}(T_R) &= 0.01869; \\ \beta^{(1)}(T_R) &= 1.0994; \\ C^\phi(T_R) &= 0.005549; \\ (\partial \beta^{(0)} / \partial T)_{(T=T_R)} &= 0.002349; \\ (\partial \beta^{(1)} / \partial T)_{T=T_R} &= 0.005958; \\ (\partial C^\phi / \partial T)_{T=T_R} &= -0.000479; \\ q_5 &= -1.03611\text{E-}5; \\ q_6 &= 3.00299\text{E-}2; \\ q_7 &= -1.43441\text{E}1 \end{aligned}$$

## Appendix D

### Dielectric constant of pure water

The relative dielectric constant of water is (Bradley and Pitzer [5]):

$$D(T, p) = U_1 \exp(U_2 T + U_3 T^2) + C(T) \ln \left( \frac{B(T) + p}{B(T) + 1000} \right) \quad (\text{D.1})$$

where

$$B(T) = U_7 + \frac{U_8}{T} + U_9 T \quad (\text{D.2})$$

$$C(T) = U_4 + \frac{U_5}{U_6 + T}. \quad (\text{D.3})$$

$$\begin{aligned} U_1 &= 3.4279\text{E}02; & U_6 &= -1.8289\text{E}02; \\ U_2 &= -5.0866\text{E-}03; & U_7 &= -8.0325\text{E}03; \\ U_3 &= 9.4690\text{E-}07; & U_8 &= 4.2142\text{E}06; \\ U_4 &= -2.0525; & U_9 &= 2.1417; \\ U_5 &= 3.1159\text{E}03 \end{aligned}$$

In these equations,  $p$  is in bars.

In the range investigated here,  $p$  was set equal to the saturation pressure of pure water.

## Appendix E

Equations for the vapor pressure  $p_w^s$  and saturated liquid density  $\rho_w^l$  of pure water

Equations given by Saul and Wagner [11]

$$\begin{aligned} q_8 &= -6.66894\text{E-}1; \\ q_9 &= -3.23550\text{E-}4; \\ q_{10} &= 5.76552\text{E-}1; \\ q_{11} &= -1.88769\text{E}2; \\ q_{12} &= -2.05974\text{E-}1; \\ q_{13} &= 1.46744\text{E}3; \\ q_{14} &= 5.14316\text{E-}5; \\ q_{15} &= 3.45791\text{E-}1; \end{aligned}$$

$$\ln \left( \frac{p_w^s}{p_c} \right) = \frac{T_c}{T} (a_1 \theta + a_2 \theta^{1.5} + a_3 \theta^3 + a_4 \theta^{3.5} + a_5 \theta^4 + a_6 \theta^{7.5}) \quad (\text{E.1})$$

$$\frac{\rho_w^l}{\rho_c} = 1 + b_1 \theta^{(1/3)} + b_2 \theta^{(2/3)} + b_3 \theta^{(5/3)} + b_4 \theta^{(16/3)} + b_5 \theta^{(43/3)} + b_6 \theta^{(110/3)} \quad (\text{E.2})$$

where

$$\theta = 1 - \frac{T}{T_c}. \quad (\text{E.3})$$

$$\begin{aligned}
 a_1 &= -7.85823; & b_1 &= 1.99206; \\
 a_2 &= 1.83991; & b_2 &= 1.10123; \\
 a_3 &= -11.7811; & b_3 &= -0.512506; \\
 a_4 &= 22.6705; & b_4 &= -1.75263; \\
 a_5 &= -15.9393; & b_5 &= -45.4485; \\
 a_6 &= 1.77516; & b_6 &= -6.75615E05
 \end{aligned}$$

Critical properties of water:  $p_c = 22.064$  MPa,  
 $T_c = 647.14$  K,  $\rho_c = 322.0$  kg/m<sup>3</sup>.

## References

- [1] H. Hasse and G. Maurer, *Ber. Bunsenges. Phys. Chem.*, 96 (1992) 83–96.
- [2] F. Weyrich, *Untersuchungen zum kalorischen Verhalten von Gemischen aus Ammoniak, Kohlendioxid, starken Elektrolyten und Wasser*. Ph-D. Dissertation, Universität Kaiserslautern, 1997.
- [3] K.S. Pitzer, *J. Phys. Chem.*, 77 (1973) 268–277.
- [4] P.S.Z. Rogers and K.S. Pitzer, *J. Phys. Chem.*, 85 (1981) 2886–2895.
- [5] D.J. Bradley and K.S. Pitzer, *J. Phys. Chem.*, 83 (1979) 1599–1603.
- [6] H.P. Snipes, C. Manly and D.D. Ensor, *J. Chem. Eng. Data*, 20 (1975) 287–291.
- [7] K.S. Pitzer, *Activity coefficients in electrolyte solutions*, 2nd edn., CRC Press, Boca Raton, 1991.
- [8] B.P. Nikolski, *Handbuch des Chemikers*, Vol. 3, VEB-Verlag Technik, Berlin, 1959.
- [9] S.L. Clegg, S. Milioto and D.A. Palmer, *J. Chem. Eng. Data*, 41 (1996) 455–467.
- [10] B. Rumpf and G. Maurer, *Ind. Eng. Chem. Res.*, 32 (1993) 1780–1789.
- [11] A. Saul and W. Wagner, *J. Phys. Chem. Ref. Data*, 16 (1987) 893–901.
- [12] S.W. Brelvi and J.P. O'Connell, *AIChE J.*, 18 (1972) 1239–1243.
- [13] T.M. Smolen, D.B. Manley and B.E. Poling, *J. Chem. Eng. Data*, 36 (1991) 202–208.
- [14] R.A. Macriss, B.E. Eakin, R.T. Ellington and J. Huebler, *Physical and thermodynamic properties of ammonia–water mixtures*, Institute of Gas technology, Research Bulletin No. 34, 1964.
- [15] G. Scatchard, L.F. Epstein, J. Warburton and P.J. Cody, *J. Am. Soc. Refrig. Eng.*, 53 (1947) 413–419.
- [16] H. J. Staudt, *Experimentelle Bestimmung und Korrelation der Exzeßenthalpie und des Exzeßvolumens binärer wäßriger Amin- und Alkoholsysteme sowie des Systems Ammoniak–Wasser in Abhängigkeit von Druck, Temperatur und Zusammensetzung*. Ph-D. Dissertation, Universität Kaiserslautern, 1984.
- [17] J. D'Ans and E. Lax, *Taschenbuch für Chemiker und Physiker*. Vol. 1, 3. edn., Springer Verlag, Berlin, 1964.
- [18] *Landolt-Börnstein, Zahlenwerte und Funktionen aus Physik, Chemie, Astronomie, Geophysik und Technik*. Vol. 2, 6. edn., Springer Verlag, Berlin, 1977.